

# High-Performance Emission/Color Dual-Switchable Polymer-Bearing Pendant Tetraphenylethylene (TPE) and Triphenylamine (TPA) Moieties

Ningwei Sun,<sup>†,‡</sup> Kaixin Su,<sup>†</sup> Ziwei Zhou,<sup>‡</sup> Xuzhou Tian,<sup>†</sup> Zhao Jianhua,<sup>§</sup> Danming Chao,<sup>†,§</sup> Daming Wang,<sup>†</sup> Franziska Lissel,<sup>\*,‡</sup> Xiaogang Zhao,<sup>\*,†,§</sup> and Chunhai Chen<sup>\*,†</sup>

<sup>†</sup>Key Laboratory of High Performance Plastics (Jilin University), Ministry of Education, National & Local Joint Engineering Laboratory for Synthesis Technology of High Performance Polymer, College of Chemistry, Jilin University, Changchun 130012, P. R. China

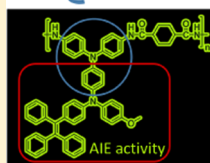
<sup>‡</sup>Leibniz Institut für Polymerforschung Dresden e.V., D-01069 Dresden, Germany

<sup>§</sup>Institute of Building Science and Technology, School of Architecture, Tianjin University, Tianjin 300072, P. R. China

## Supporting Information

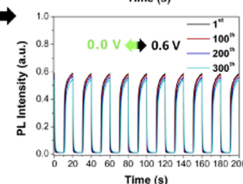
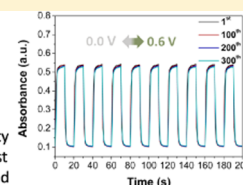
**ABSTRACT:** Electrofluorochromic (EFC) materials have aroused great interest owing to their interesting ability of tuning fluorescence in response to the applied potential. However, some crucial characteristics, such as response speed, fluorescence contrast, and switching stability, are still not well realized to meet the requirements of practical applications. Herein, we designed and synthesized a novel polyamide-bearing aggregation-induced emission (AIE)-active tetraphenylethylene (TPE) and a highly conjugated triphenylamine (TPA) pendant group. The rational combination of the highly conjugated TPA and TPE caused the resultant polymer to exhibit highly integrated electrochromic (EC) and EFC performances including multiple color-changing (colorless to green to blue), fast response speed (1.8/1.1 s for EC and 0.4/2.9 s for EFC process), high fluorescence contrast (82 at the duration time of 20 s), and excellent long-term stability over 300 cycles. The strategy of AIE functionality by combing a highly conjugated redox unit demonstrates a synergistic effect to prepare high-performance emission/color dual-switchable materials, greatly promoting their applications in sensors, smart windows, and displays.

Highly stable electrochemistry properties of the first redox



Twisted and bulky side group

- Excellent stability
- High optical contrast
- Fast response speed



## INTRODUCTION

Switchable fluorescence materials have drawn great attentions due to their potential applications in the fields of sensors, informational displays, encryption, and memory devices.<sup>1–8</sup> However, conventional fluorescent materials exhibiting strong emission in solution always suffer from serious quenching problems when utilized as solid film or nanoparticles, which greatly restricted their real-life applications.<sup>9–11</sup> To circumvent this urgent problem, numerous efforts have been made to prevent aggregations including dendritic substituent protection, introduction of bulky groups, and blending of transparent polymers.<sup>12–17</sup> But in many cases, these approaches have met with limited success because the aggregations are only prevented temporarily or partially. It would be of great significance if a system could be developed in which the aggregation would promote rather than quench fluorescence. In 2001, Tang et al. reported an interesting hexaphenylsilole molecule exhibiting aggregation-induced emission (AIE), i.e., being nonluminescent in solution state but emissive in aggregated state.<sup>18</sup> This special phenomenon not only raises interesting academic questions but also shows great promise

for practical applications; by now, a number of AIE-active organic fluorophores have been developed and explored. Among various AIE luminogens, tetraphenylethylene (TPE) with four rotatable phenyl rings is a prototypical molecule and has been well-investigated.<sup>19–23</sup> The TPE structure can be easily modified in a versatile way, enabling a facile introduction into various switchable fluorescence systems to dramatically improve the fluorescence contrast in the solid state.

On the other hand, triphenylamine (TPA) derivatives are well known for their interesting electroactive and photoactive properties and have been extensively applied in dye-sensitized solar cells, light emitters, and electrochromic (EC) devices.<sup>24–30</sup> Electron-donating TPA can be easily oxidized to cation radicals (TPA<sup>+</sup>), making it a promising candidate as the electroactive modulator. Following this reasoning, the judicious combination of TPA and fluorophores is expected to give highly functional materials that could simultaneously realize

**Received:** January 13, 2019

**Revised:** May 17, 2019

color and emission dual switching, beneficial for the development of dual-mode displays.<sup>31–36</sup> However, while several TPA-based emission/color dual-switchable materials have been developed, most of them usually have limited response speed, moderate cycling stability, and low fluorescence contrast, which greatly hindered their further applications. To address the problem of low fluorescence contrast, AIE functionality is an effective method. Following this strategy, we have recently reported an electro-/AIE-active polymer with the diphenylamine–TPE unit, showing the highest fluorescence on/off contrast so far.<sup>37</sup> The fluorescence contrast could be readily improved; nevertheless, the response speed and long-term stability are still not well-realized simultaneously. Thus, a further optimized molecular design for the fabrication of high-performance emission/color dual-switchable is required. Remarkably, a highly conjugated TPA derivative, tetraphenyl-*p*-phenylenediamine, was found to possess an increased highest occupied molecular orbital level and thus reduced oxidation potential as well as superior electrochemical stability.<sup>38</sup> The EC polymers with tetraphenyl-*p*-phenylenediamine moieties revealed excellent switching stability up to thousands of cycles.<sup>39,40</sup> Furthermore, the highly conjugated tetraphenyl-*p*-phenylenediamine can significantly enhance the intramolecular charge mobility, helping to increase the response speed. Therefore, combing AIE-active TPE with stable electroactive tetraphenyl-*p*-phenylenediamine will be a rational strategy to synergistically improve the EC and EFC performances.

Herein, we designed and synthesized a novel electro-/AIE-active polymer with a bulky and asymmetric pendant group constructed by TPE and TPA moieties. Introduction of TPE is expected to enhance the fluorescence in the solid state and improve the fluorescence on/off contrast. The highly conjugated TPA structure is responsible for providing a stable electrochemical modulator to switch the dual emission and color. Furthermore, the bulky pendant substituent and the highly conjugated TPA will function together to shorten the response time. The carefully devised polymer can highly integrate the excellent performances of emission/color switching, including high contrast, outstanding switching stability, and fast response speed (Figure 1).

## EXPERIMENTAL SECTION

**Materials.** 4-Bromobenzophenone (TCI), benzophenone (TCI), *p*-phenylenediamine (TCI), 4-fluoronitrobenzene (Acros), trimethylamine (Aladdin), TiCl<sub>4</sub> (TCI), zinc (Zn, Acros), potassium carbonate (K<sub>2</sub>CO<sub>3</sub>), copper powder (Acros), 10% palladium on charcoal (Pd/C,

Aladdin), and 80% hydrazine monohydrate (Aladdin) were used without further treatment. Commercially available 1,4-cyclohexanedicarboxylic acid (CHDA, Sigma-Aldrich) was dried in a vacuum oven at 100 °C prior to use. Dimethyl sulfoxide (DMSO), *N*-methyl-2-pyrrolidinone (NMP), *o*-dichlorobenzene, pyridine (Py, Aladdin), and triphenyl phosphite (TPP, TCI) were treated using 4 Å molecular sieves before using. Tetrabutylammonium perchlorate (TBAP, TCI) was purified by recrystallization from ethanol and dried in a vacuum oven prior to use. All other chemicals were directly used as received.

**Synthesis of 4-Methoxy-4'-nitrodiphenylamine (1).** 4-Methoxy-4'-nitrodiphenylamine **1** was obtained following a reported method in the previous work.<sup>41</sup> <sup>1</sup>H NMR (300 MHz, DMSO-*d*<sub>6</sub>, δ, ppm): 9.11 (s, 1H), 8.06 (d, *J* = 9.3 Hz, 2H), 7.17 (d, *J* = 8.9 Hz, 2H), 6.97 (d, *J* = 9.0 Hz, 2H), 6.89 (d, *J* = 9.3 Hz, 2H), 3.75 (s, 3H).

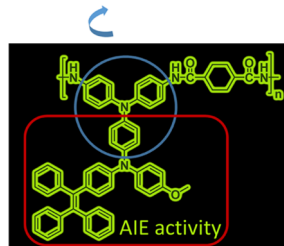
**Synthesis of 1-Bromo-4-(1,2,2-triphenylethenyl)benzene (2).** 1-Bromo-4-(1,2,2-triphenylethenyl)benzene **2** was synthesized through the McMurry reaction.<sup>42</sup> A suspension solution was obtained by adding Zn powder (15.0 g, 231.3 mmol) to anhydrous tetrahydrofuran (THF) (650 mL) under the argon atmosphere, which was cooled to –5 °C. Then, TiCl<sub>4</sub> (12.7 mL, 115.6 mmol) was slowly added into the solution with a syringe. The above mixture was heated for 3 h at the reflux temperature. Subsequently, the solution was cooled to –5 °C, into which pyridine (7.5 mL) was added, and the solution was further stirred for 0.5 h. Then, benzophenone (7.5 g, 41.1 mmol) and 4-bromobenzophenone (8.6 g, 33.1 mmol) in 50 mL of THF were added slowly, and the reaction was further proceeded for 12 h at the reflux temperature. The above reaction was quenched by adding 10% K<sub>2</sub>CO<sub>3</sub> aqueous solution and extracted by dichloromethane for three times. The crude was purified by chromatography to get the desired products (7.6 g, yield 55%). <sup>1</sup>H NMR (300 MHz, DMSO-*d*<sub>6</sub>): 7.38 (d, *J* = 8.4 Hz, 2H), 7.34 (d, *J* = 8.4 Hz, 2H), 7.22–7.10 (m, 7H), 7.01–6.87 (m, 8H).

**Synthesis of 4-Nitrophenyl-4-methoxyphenyl-4-animo-tetraphenylethylene (3).** 4-Nitrophenyl-4-methoxyphenyl-4-animo-tetraphenylethylene **3** was synthesized through the Ullmann coupling reaction. A mixture of **2** (5 g, 12.1 mmol), **1** (3.3 g, 13.4 mmol), copper powder (3.0 g, 48.4 mmol), 18-crown-6 ether (1.6 g, 6.1 mmol), potassium carbonate (6.7 g, 48.4 mmol), and *o*-dichlorobenzene (30 mL) was heated at 170 °C for 20 h under a N<sub>2</sub> atmosphere. The insoluble solids were immediately filtered from the mixture. Then, the solvent, *o*-dichlorobenzene, was removed from the filtrate under vacuum distillation. The resulting crude material was further purified by recrystallization to afford 5.1 g of mononitro compound **3** (yield: 74%). Fourier-transform infrared spectroscopy (FTIR) (KBr): 1306, 1586 cm<sup>–1</sup> (–NO<sub>2</sub> stretch). <sup>1</sup>H NMR (300 MHz, DMSO-*d*<sub>6</sub>, δ, ppm): 8.04 (d, *J* = 9.4 Hz, 2H), 7.22–7.09 (m, 11H), 7.06–6.95 (m, 12H), 6.66 (d, *J* = 9.3 Hz, 2H), 3.77 (s, 3H).

**Synthesis of 4-Aminophenyl-4-methoxyphenyl-4-animo-tetraphenylethylene (4).** 4-Aminophenyl-4-methoxyphenyl-4-animo-tetraphenylethylene **4** was obtained by a Pd/C-catalyzed reduction. A mixture of **3** (5.0 g, 8.7 mmol) and 10% Pd/C (0.6 g) was dispersed in 80 mL of dioxane and then heated to reflux. Hydrazine monohydrate (8 g) was subsequently added to the above mixture, which reacted at 100 °C for another 6 h. Then, Pd/C was removed by immediate filtration. The resulting filtrate was slowly poured into 100 mL of stirred water to afford a pale yellow powder. The powder was collected and dried in a vacuum oven at 70 °C, giving 3.6 g of monoamino compound **4** (yield: 77%). FTIR (KBr): 3368, 3460 cm<sup>–1</sup> (–NH<sub>2</sub> stretch). <sup>1</sup>H NMR (300 MHz, DMSO-*d*<sub>6</sub>, δ, ppm): 7.21–7.05 (m, 9H), 7.01–6.90 (m, 8H), 6.84 (d, *J* = 9.0 Hz, 2H), 6.75 (d, *J* = 8.6 Hz, 2H), 6.68 (d, *J* = 8.7 Hz, 2H), 6.51 (d, *J* = 8.6 Hz, 2H), 6.42 (d, *J* = 8.8 Hz, 2H), 5.20 (s, 2H), 3.70 (s, 3H).

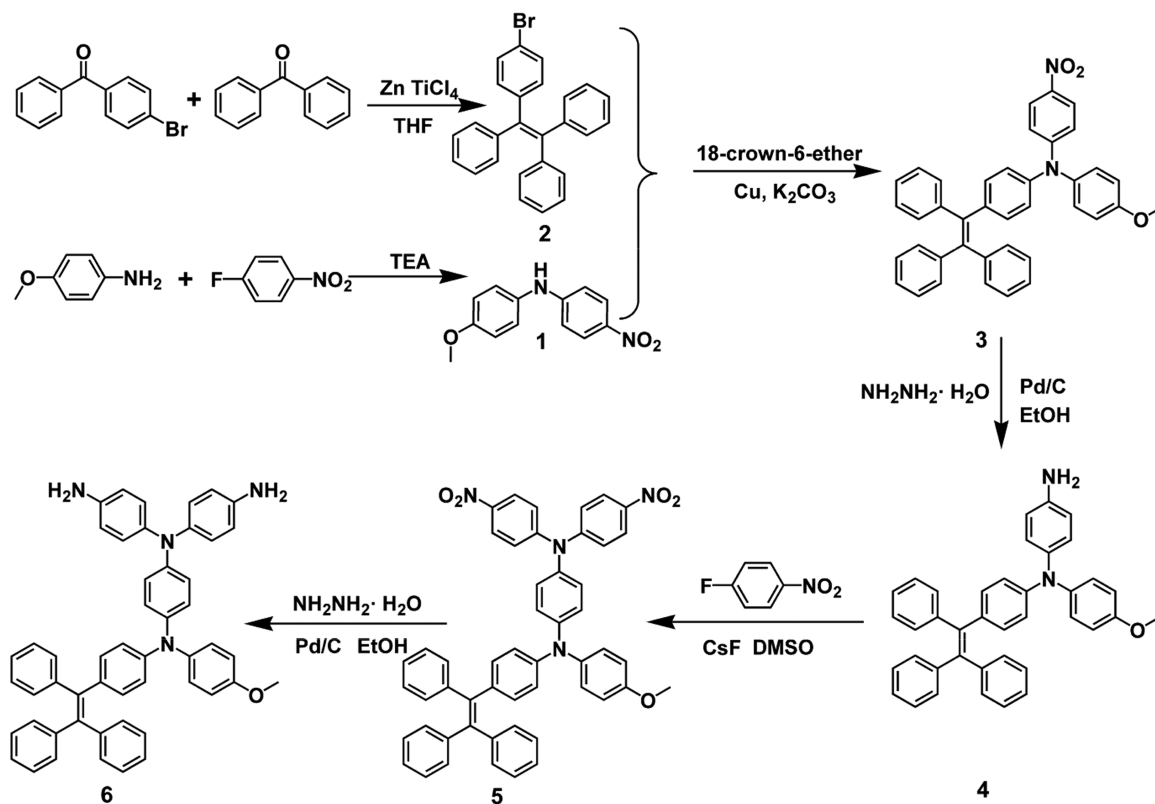
**Synthesis of *N,N*-Bis(4-nitrophenyl)-*N'*-4-methoxyphenyl-*N'*-4-(1,2,2-triphenylethenyl)phenyl-1,4-phenylenediamine (5).** *N,N*-Bis(4-nitrophenyl)-*N'*-4-methoxyphenyl-*N'*-4-(1,2,2-triphenylethenyl)-phenyl-1,4-phenylenediamine **5** was synthesized through a nucleophilic substitution reaction. In a 250 mL flask, 3.0 g (5.5 mmol) of **4**, 1.6 g (11.5 mmol) of 4-fluoronitrobenzene, and 1.8 g (11.5 mmol) of CsF were added in 15 mL of DMSO. Then, the mixture was stirred at 145 °C for 12 h, which was cooled and poured into 300 mL of stirred

Highly stable electrochemistry  
properties of the first redox



Twisted and bulky side group

**Figure 1.** Design concept of a novel electro-/AIE-active polymer with TPE and highly conjugated TPA units.

Scheme 1. Synthetic Route of a Novel Diamine **6** with TPE and TPA Units

ethanol to afford a red solid powder. The resulting crude powder was recrystallized twice from DMAc/ethanol to give 3.0 g of dinitro compound **5** (yield: 71%). FTIR (KBr): 1307, 1575  $\text{cm}^{-1}$  ( $-\text{NO}_2$  stretch).  $^1\text{H NMR}$  (300 MHz,  $\text{DMSO}-d_6$ ,  $\delta$ , ppm): 8.18 (d,  $J = 9.3$  Hz, 4H), 7.21 (d,  $J = 9.2$  Hz, 4H), 7.19–6.92 (m, 21H), 6.90 (d,  $J = 2.3$  Hz, 2H), 6.87 (d,  $J = 2.2$  Hz, 2H), 6.80 (d,  $J = 8.6$  Hz, 2H), 3.75 (s, 3H).

**Synthesis of *N,N*-Bis(4-aminophenyl)-*N'*-4-methoxyphenyl-*N'*-4-(1,2,2-triphenylethenyl)phenyl-1,4-phenylenediamine (**6**).** *N,N*-Bis(4-aminophenyl)-*N'*-4-methoxyphenyl-*N'*-4-(1,2,2-triphenylethenyl)phenyl-1,4-phenylenediamine **6** was synthesized by reduction of dinitro compound **5**. In a 250 mL round-bottom flask, **5** (2.5 g, 3.2 mmol) and 10% Pd/C (0.8 g) was dispersed in 60 mL of dioxane and then heated to reflux. Into the above mixture, 6 g of hydrazine monohydrate was subsequently added and stirred at the reflux temperature for another 12 h. Then, Pd/C was immediately removed by filtration, and the obtained filtrate was cooled under a nitrogen flow to slowly precipitate yellow powder, which was collected and dried in a vacuum oven (1.8 g with a yield of 78%). FTIR (KBr): 3371, 3457  $\text{cm}^{-1}$  ( $-\text{NH}_2$  stretch).  $^1\text{H NMR}$  (600 MHz,  $\text{DMSO}-d_6$ ,  $\delta$ , ppm): 7.17 (t,  $J = 7.4$  Hz, 2H,  $\text{H}_a$ ), 7.16–7.04 (m, 7H,  $\text{H}_{i+j+k}$ ), 7.02–6.95 (m, 4H,  $\text{H}_m$ ), 6.94 (m, 4H,  $\text{H}_{h+i}$ ), 6.87 (d,  $J = 9.0$  Hz, 2H,  $\text{H}_g$ ), 6.80 (d,  $J = 8.7$  Hz, 4H,  $\text{H}_b$ ), 6.77 (d,  $J = 6.6$  Hz, 2H,  $\text{H}_e$ ), 6.71 (d,  $J = 8.8$  Hz, 2H,  $\text{H}_d$ ), 6.55 (d,  $J = 9.0$  Hz, 2H,  $\text{H}_f$ ), 6.52 (d,  $J = 8.6$  Hz, 4H,  $\text{H}_3$ ), 6.48 (d,  $J = 8.8$  Hz, 2H,  $\text{H}_c$ ), 4.95 (s, 4H,  $-\text{NH}_2$ ), 3.71 (s, 3H,  $-\text{OCH}_3$ ).

**Synthesis of the Polyamide with TPE and TPA Units.** Following the phosphorylation technique,<sup>43</sup> a polyamide-containing TPE fluorophore and tetraphenyl-*p*-phenylenediamine electroactive unit was prepared as follows. The newly synthesized diamine **6** (0.7263 g, 1 mmol), CHDA (0.172 g, 1 mmol), TPP (1 mL), Py (0.5 mL), and calcium chloride (0.1 g) were added to 2.0 mL of NMP. The reaction system was then heated with stirring at 120 °C for 3 h. The resulting viscous solution was cooled and precipitated in 500 mL of methanol with vigorously stirring. The resultant fiberlike polymer solid was collected by filtration and washed with lots of methanol and hot water. Additionally, further purification was proceeded by reprecipi-

tation of the polymer from DMAc into ethanol. FTIR (KBr): 3325, 1674  $\text{cm}^{-1}$  (amide group).  $^1\text{H NMR}$  (300 MHz,  $\text{DMSO}-d_6$ ,  $\delta$ , ppm) 9.73 (s, 2H), 7.50 (d,  $J = 8.9$  Hz, 4H), 7.21–7.05 (m, 11H), 7.03–6.94 (m, 8H), 6.94–6.86 (m, 6H), 6.84–6.80 (m, 4H), 6.77 (d,  $J = 8.7$  Hz, 2H), 6.59 (d,  $J = 8.7$  Hz, 2H).

**Measurements.** NMR spectra were collected on a BRUKER-300 spectrometer. Fourier transform infrared (FTIR) spectra were recorded through a Bruker Vector 22 spectrometer. Gel permeation chromatographic (GPC) data was collected from a PL-GPV 220 instrument using dimethylformamide (DMF) as an eluent (flow rate: 1.0 mL/min). Thermogravimetric analysis (TGA) was obtained on the TA 2050 at a heating rate of 10 °C/min. Differential scanning calorimetric (DSC) analysis was carried out on TA Q100 at a scanning rate of 10 °C/min using 50 mL/min nitrogen flow. CHI 660e electrochemical workstation was used for the electrochemical measurements. Cyclic voltammetry (CV) tests were conducted using polymer film/indium-tin oxide (ITO) as a working electrode, a Ag/AgCl, KCl (sat.) as a reference electrode, and a platinum wire as an auxiliary electrode. UV–vis–NIR spectra were collected with a Shimadzu UV 3101-PC spectrophotometer. Fluorescence spectra were recorded using an Edinburgh FLS920 fluorescence spectrophotometer. The spectro-electrochemical cell was composed of a quartz cell with a three-electrode system. The EC and EFC switching properties were measured by coupling an electrochemical workstation with an UV–vis and fluorescence spectrophotometer. That way, the absorption and emission changes under the potential control could be obtained. The switching time was calculated at 95% of the full optical switching, as it is hard to perceive any further optical changes by naked eyes beyond this point. The fluorescence on/off contrast was calculated as the high fluorescence value at the neutral state ( $I_{\text{off}}$ )/the low fluorescence value at the highest applied potential ( $I_{\text{on}}$ ).

## RESULTS AND DISCUSSION

**Synthesis and Characterization of the Monomers and the Polyamide.** A new diamine with AIE-active TPE and highly conjugated tetraphenyl-*p*-phenylenediamine moieties

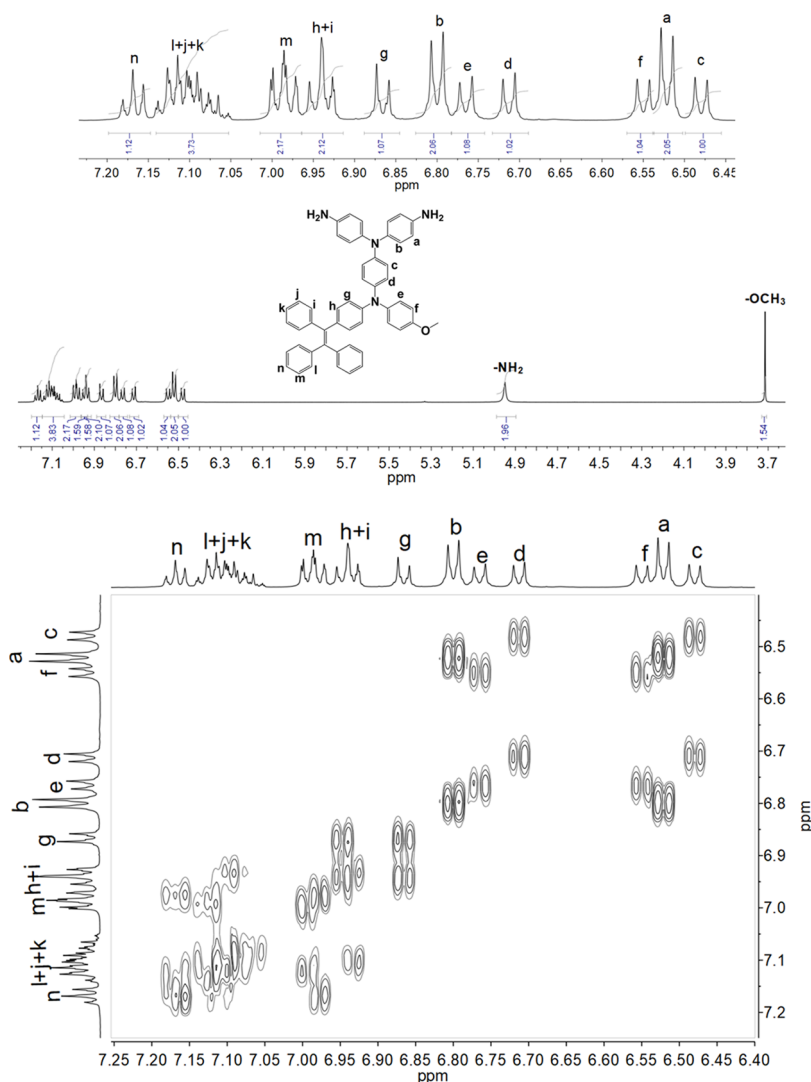
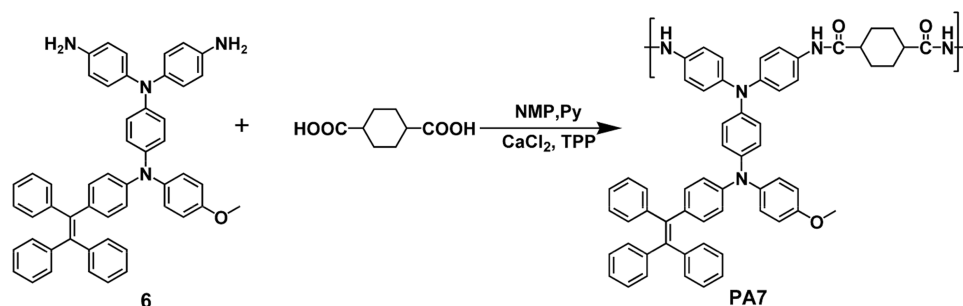


Figure 2.  $^1\text{H}$  NMR (top) and H–H COSY (bottom) spectra of diamine **6**.

### Scheme 2. Synthesis of the Electro-/AIE-Active Polyamide PA7



was rationally designed and synthesized via a six-step route (Scheme 1). Diphenylamine **1** was obtained from an amination reaction of *p*-phenylenediamine and 4-fluoronitrobenzene. Brominated TPE **2** was synthesized by a McMurry reaction from benzophenone and 4-bromobenzophenone. Then, the Ullmann reaction of **1** and **2** gave the mononitro compound **3**, which was reduced to the monoamino compound **4** by means of Pd/C and hydrazine. The dinitro compound **5** was obtained from the CsF-assisted nucleophilic substitution reaction of **4** with two-equivalent 4-fluoronitrobenzene. The objective diamine **6** was successfully synthesized by the hydrazine Pd/

C-catalyzed reduction of **5**. The chemical structures of the prepared monomers were analyzed and identified by FTIR and NMR spectra. The FTIR spectra are summarized in Figure S1, from which we could see that the diamine **6** gave characteristic stretching absorption pairs of amino groups at 3371 and 3457  $\text{cm}^{-1}$ . The  $^1\text{H}$  NMR spectrum of the target diamine **6** is illustrated in Figure 2 with the assignments of all proton signals assisted by the COSY spectrum (the  $^1\text{H}$  NMR spectra of the intermediate monomers **1**–**5** are summarized in Figure S3). All of the resonance signals are well-matched with the protons of the proposed molecular structure, proving that the new

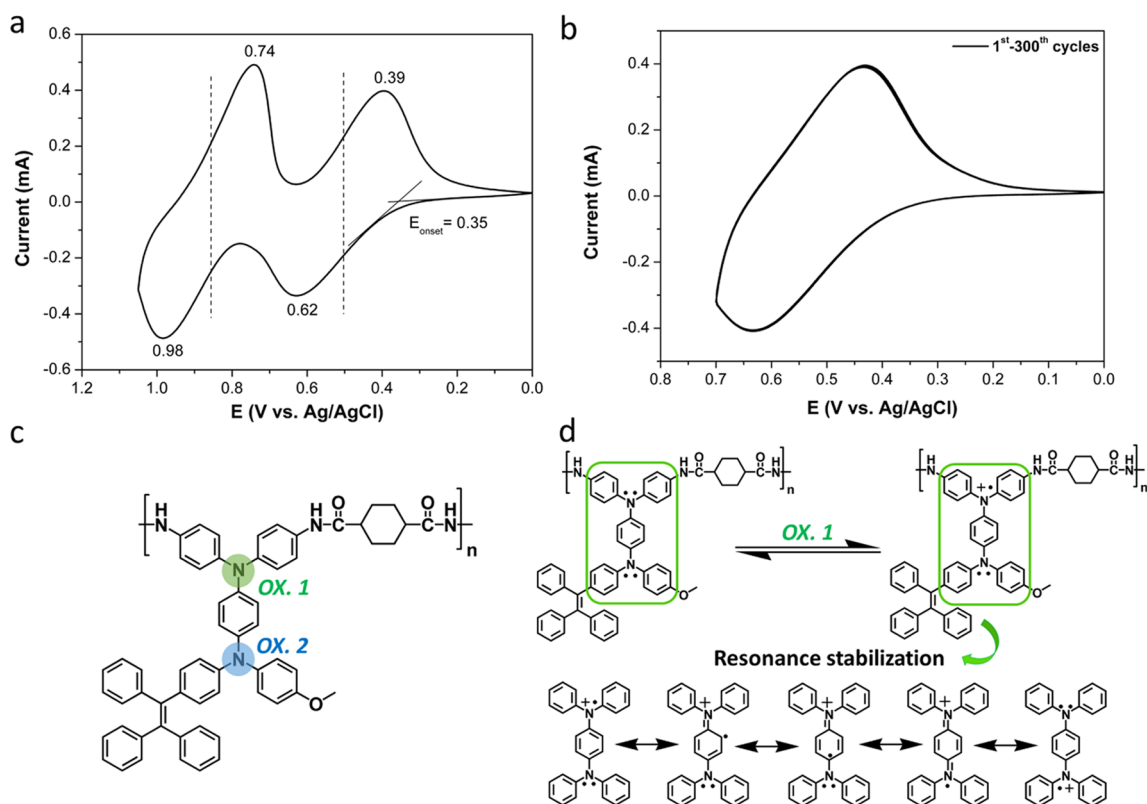


**Figure 3.** CV diagrams of PA7 from 0.0 to 1.2 V (a) and from 0.0 to 0.7 V for continuous 300 cycles (b). Oxidation order of the nitrogen centers (c). Resonance stabilization forms of the cation radical (d).

diamine **6** has been successfully synthesized. After obtaining the pure diamine **6**, the judiciously designed AIE-active TPE and the highly conjugated TPA structures could be readily introduced to the polyamide through the phosphorylation technique (Scheme 2). The resulting polyamide was abbreviated to PA7 whose structure was also validated by FTIR and NMR spectra. The FTIR spectrum of PA7 (Figure S2) revealed amide stretching absorption bands at  $1674\text{ cm}^{-1}$  (C=O) and  $3325\text{ cm}^{-1}$  (N–H). In Figure S3, the  $^1\text{H}$  NMR spectrum of PA7 agreed well with the target structure of a polyamide repeat unit. Accordingly, these results indicate that the novel electro-/AIE-active polyamide with highly conjugated TPA and TPE moieties has been successfully prepared.

For further revealing the physical properties of PA7, its inherent viscosity, molecular weight, solubility, and thermal properties were comprehensively investigated. PA7 had an inherent viscosity of 0.93 and could be easily solution-cast to obtain free-standing films, indicating a high molecular weight of PA7. The number-average molecular weights and the polydispersity of PA7 were subsequently tested with GPC, which were found to be 45 900 and 1.37, respectively. The solubility behavior was evaluated at 10% w/v concentration in common organic solvents with the results summarized in Table S1. PA7 is highly soluble in polar solvents including NMP, DMAc, DMF, and DMSO due to the introduction of bulky and twisty tetraphenyl-*p*-phenylenediamine and TPE units, decrease in the interchain interactions, and increase in the free volume of the polymer chains. Moreover, the thermal properties of PA7 were studied by TGA and DSC analysis. PA7 revealed a high thermal stability with a 10% weight loss at  $451\text{ }^\circ\text{C}$ , and the glass transition temperature was found to be up to  $226\text{ }^\circ\text{C}$ . The excellent solubility, thermal stability, and

film-forming property are all important for further applications in the flexible optoelectronic devices.

**Electrochemical, Spectro-Electrochemical, and Electrochromic Properties.** After the introduction of the highly conjugated TPA electroactive unit, the electrochemical behavior of the as-prepared polymer PA7 was investigated by CV measurements, using the polymer film/ITO substrates as the working electrodes and 0.1 M TBAP in acetonitrile as the supporting electrolyte. The CV diagrams in Figure 3a exhibit two quasi-reversible redox couples at 0.62/0.39 V and 0.98/0.74 V, corresponding to the electrons successively removed from two different nitrogen centers. The first electron removal occurred at the nitrogen atom on the main chains because of the higher electron density compared with the nitrogen atom on the pendant TPE–diphenylamine unit (Figure 3c). Benefiting from the highly conjugated tetraphenyl-*p*-phenylenediamine structure, the polymer PA7 exhibited a low driving potential with an onset oxidation potential of as low as 0.35 V. Due to the low redox potential as well as the resonance stabilization of the cation radical (Figure 3d), the first redox process exhibits a very high electrochemical stability. As shown in Figure 3b, the CV scans from 0.0 to 0.7 V reveal a highly stable redox process in continuous 300 cycles without an obvious decrease in the peak current, which will be very valuable as an electrochemical modulator.

There were visual color changes during the CV test, and thus the EC behavior was further manifested by the spectroelectrochemical measurements. For the investigation, the spectra of the polymer film coated on ITO substrate were collected in situ by a UV–vis spectrophotometer under the potentials control of an electrochemistry workstation. As shown in Figure 4a, PA7 showed a strong absorption band at

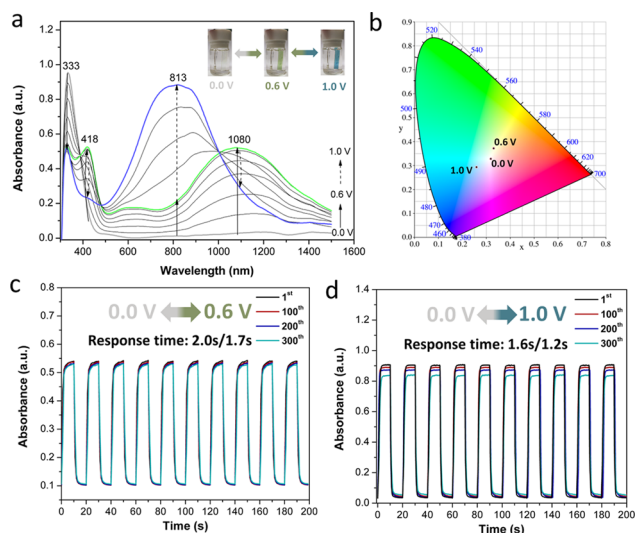


**Figure 4.** (a) Absorbance spectra of PA7 thin-film electrode in 0.1 M TBAP/CH<sub>3</sub>CN at different applied potentials from 0.0 to 1.0 V. (b) CIE chromaticity at different potentials (0.0 V Yxy: 65.06, 0.3183, 0.3284; 0.6 V Yxy: 45.60, 0.3312, 0.3717; 1.0 V Yxy: 33.51, 0.2585, 0.2934). (c) EC switching between 0.0 and 0.6 V for the first color-changing process (coloring/bleaching: 2.0/1.7 s). (d) EC switching between 0.0 and 1.0 V for the second color-changing process (coloring/bleaching: 1.6/1.2 s).

333 nm in the neutral state. Upon oxidation by steadily increasing potentials from 0.0 to 0.6 V, the intensity of the neutral absorption at 333 nm gradually decreased while two new absorption bands at 418 and 1080 nm increased in intensity, which could be attributed to the formation of TPA<sup>+</sup> on the main chain. The electron delocalization over the two nitrogen centers leads to an intervalence charge-transfer absorption in the near-infrared region.<sup>39</sup> With the potential adjusted from 0.6 to 1.0 V, to achieve a complete oxidation of the two nitrogen centers, the absorption bands at 418 and 1080 nm decreased with one new peak at 813 nm grown up gradually. As seen in the inset in Figure 4a, the polymer film changed from colorless in the neutral state (CIE Yxy: 65.06, 0.3183, 0.3284) to green for the first oxidation state (CIE Yxy: 45.60, 0.3312, 0.3717) and then to blue for the second oxidation state (CIE Yxy: 33.51, 0.2585, 0.2934). The EC characteristics of switching stability and response time were investigated by monitoring the absorption changes when applying potential steps in the kinetics studies. Figure 4c,d demonstrates the EC switching stability for the two redox procedures, respectively. For the first EC switching between 0.0 and 0.6 V, PA7 exhibited highly stable states and full reversibility without an obvious decay in continuous 300 cycles, benefiting from the stable redox property and the good adhesion between the polymer thin film and the ITO substrate. For the second EC process between 0.0 and 1.0 V, the switching stability was found to be poorer in comparison with the first EC process, which showed about 9.1% decay of the optical contrast after 300 cycles. Regarding the second EC process, the side reactions caused by the applied high voltage may be responsible for the decreased cyclic stability. Moreover, the response time (coloring/bleaching) calculated at 95% of the full optical changes was found to be 2.0/1.7 s and 1.6/1.2 s for the first and second EC processes, respectively. Compared with the structures of other TPA-based EC polymers,<sup>28,46</sup> the lower response time of PA7 could be ascribed to the

introduction of the bulky and twisty pendant group and the highly conjugated TPA unit, preventing the close packing of polymer chains and promoting the charge transport in inter-/intramolecular chains.

**Fluorescence and EFC Properties.** TPE is a well-known AIE-active fluorophore. Combining this structural component with the electron-donating TPA unit is expected to further improve the fluorescence. Consequently, the interesting optical properties of PA7 were further investigated regarding the fluorescence and EFC switching. In Figure 5a, PA7 exhibited a

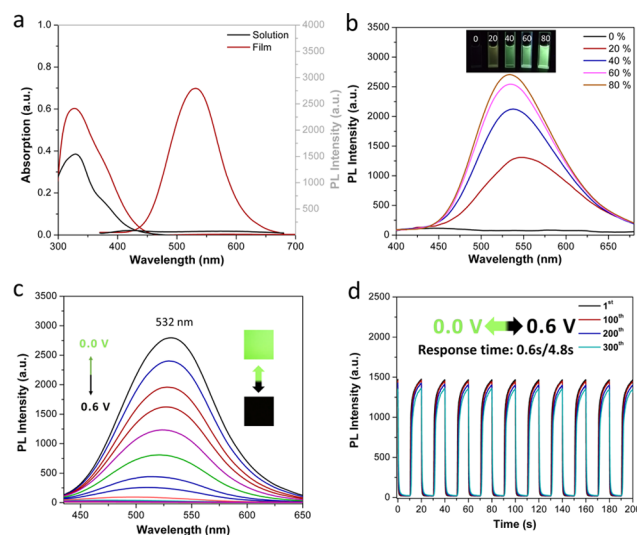


**Figure 5.** (a) UV-vis and fluorescence spectra of PA7 in the NMP solution and film states. (b) Fluorescence spectra of TPE-PDA-PA in NMP-water mixtures with different water contents (inset: fluorescence images in NMP-water mixtures). (c) Fluorescence spectra of TPE-PDA-PA film at different applied potentials. (d) Fluorescence switching response under applied potentials between 0.0 and 0.6 V at the cycling time of 20 s for 300 cycles (on/off: 0.6/4.8 s).

strong absorption at 333 and 334 nm in both solution and film states owing to the  $\pi$ -conjugated moieties of TPE and TPA in the PA7 backbone. The polymer solution emitted a rather weak fluorescence (fluorescence quantum yield: 0.6%), while the polymer film emitted an enhanced fluorescence (fluorescence quantum yield: 29.3%), demonstrating an obvious AIE activity. As shown in Figure 5b, with water, working as a poor solvent for PA7, gradually increased from 0 to 80%, the fluorescence intensity of the NMP-water mixtures enhanced significantly. The mechanism of the fluorescence enhancement has been well-illustrated by Tang, which is attributed to the restricted intramolecular rotation effect.<sup>19,47</sup> The multiple rotational phenyl rings on the TPA and TPE units dissipate the excited-state energy by intramolecular rotations in the solution state (Figure S6). However, in the aggregated state, the intramolecular rotations are restricted, activating and promoting the radiative pathway. Moreover, the highly twisted structure of TPA and TPE efficiently hinder the intermolecular  $\pi$ - $\pi$  stacking interactions that cause emission quenching. These synergistic effects result in the observed enhanced aggregation-induced emission. Furthermore, the cation radical of PA7 with a broad absorption from 450 to 650 nm could act as an efficient fluorescence quencher due to the large overlap between absorption and emission spectra. Thus, the fluorescence of PA7 might be effectively tuned by the electrochemical redox stimulation. As shown in Figure 5c,

gradually increasing potentials from 0 to 0.6 V quenched and weakened the fluorescence accordingly. When the potential of 0.6 V was reached, the fluorescence was nearly fully quenched, meaning that the monocation radical in the first oxidation state could be chosen as a sufficient quencher. Upon applying the reverse potentials, the fluorescence recovered, indicating a reversible fluorescence response. Subsequently, the fluorescence switching behavior was studied by monitoring the fluorescence emission changes when applying square-wave potentials between 0 and 0.6 V. As shown in Figure 5d, the fluorescence switching revealed an ultrahigh stability with only a slight decay in continuous 300 cycles. The excellent cycling stability is attributed to the highly stable electrochemistry property of PA7. Furthermore, it is likely that the even more stable switching cycle performance can be realized on the optimization of the EFC devices (device package, quality of the polymer film, counter layer for charge balance, and so on).<sup>44,45</sup> Remarkably, the response time calculated at 95% of full fluorescence modulation was calculated to be 0.6 and 4.8 s for quenching and lighting processes, respectively. Combination of the bulky and twisted pendant group with the highly conjugated TPA unit is responsible for the fast response speed. The former could lead to the loose packing of polymer chains, thus accelerating the insertion/extraction of the electrolyte ions, while the latter improves the intramolecular charge mobility. The intrinsic response speed of PA7 is even faster than that of the porous polymer electrode, revealing more promising application potential.<sup>37</sup> The fluorescence on/off contrast at the duration time of 20 s was calculated to be 82, without waiting for the redox event of the TPA unit to be completed. Still, the contrast ratio is larger than that of lots of reported EFC materials,<sup>32–36,45</sup> which is attributed to the highly efficient solid-state fluorescence and the fast response speed. Although the previously reported polymers TPA–CN–TPE and TPA–OMe–TPE also contained TPA and TPE units, the TPA and TPE units were incorporated in the diamine and dicarboxylic acid structures, respectively. The strong electron-withdrawing carbonyl on the TPE unit greatly decreased the fluorescence and the fluorescence on/off contrast. In contrast, the TPA unit in the electrochemical fluorophore of PA7 works as fluorochromes and increases the fluorescence in the neutral state. When TPA was oxidized to TPA<sup>+</sup>, an electron-withdrawing unit, the fluorescence of PA7 was reduced. Thus, the fluorescence on/off contrast was increased and the fluorescence quenching process was promoted. Moreover, combining the highly conjugated TPA unit of PA7, which possess enhanced intramolecular charge mobility and the bulky pendant TPA/TPE unit, the EFC switching speed is faster than those of TPA–CN–TPE and TPA–OMe–TPE. The excellent EFC switching stability together with the high fluorescence on/off contrast and a fast response speed demonstrated a synergistic effect of AIE-active TPE and highly conjugated TPA unit for fabricating a high-performance emission/color dual-switchable polymer, greatly enriching the design strategy of the competitive smart materials.

## CONCLUSIONS

In summary, we have synthesized a novel electro-/AIE-active polymer containing TPE and tetraphenyl-*p*-phenylenediamine units. The strategy by the simultaneous introduction of AIE-active TPE and highly conjugate TPA units demonstrated a synergistic effect for the preparation of high-performance EC

and EFC materials. In addition to the excellent thermal stability, solubility, and film-forming properties, the emission/color dual-switchable polymer PA7 exhibited highly integrated performances of excellent long-term cycling stability over 300 cycles, fast response speed (1.8/1.1 s for EC and 0.4/2.9 s for EFC process), and high fluorescence on/off contrast (82 at the duration time of 20). Thus, this work opens a new pathway for developing high-performance emission/color dual-switchable materials, which will greatly stimulate and promote the creative photochemical applications.

## ASSOCIATED CONTENT

### Supporting Information

The Supporting Information is available free of charge on the ACS Publications website at DOI: 10.1021/acs.macromol.9b00079.

FTIR and NMR spectra of the synthesized monomers 1–6 and the polymer PA7; TGA/DSC curves of PA7; diagram of rotational phenyl rings on TPA and TPE units; detailed information of inherent viscosities, molecular weight, and solubility properties of PA7 (PDF)

## AUTHOR INFORMATION

### Corresponding Authors

\*E-mail: lissel@ipfdd.de (F.L.).

\*E-mail: xiaogang@jlu.edu.cn (X.Z.).

\*E-mail: cch@jlu.edu.cn (C.C.).

### ORCID

Danming Chao: 0000-0003-1324-6731

Daming Wang: 0000-0002-5046-5469

Xiaogang Zhao: 0000-0002-3356-094X

### Notes

The authors declare no competing financial interest.

## ACKNOWLEDGMENTS

D.C. graciously acknowledges the National Natural Science Foundation of China for funding (Grant No. 21774046) and Jilin Provincial Science and Technology Department, China (Grant No. 20190201075JC).

## REFERENCES

- (1) Giepmans, B. N. G.; Adams, S. R.; Ellisman, M. H.; Tsien, R. Y. The fluorescent toolbox for assessing protein location and function. *Science* **2006**, *312*, 217–224.
- (2) van de Linde, S.; Sauer, M. How to switch a fluorophore: from undesired blinking to controlled photoswitching. *Chem. Soc. Rev.* **2014**, *43*, 1076–1087.
- (3) Audebert, P.; Miomandre, F. Electrofluorochromism: from Molecular Systems to Set-up and Display. *Chem. Sci.* **2013**, *4*, 575–584.
- (4) Ma, Q.; Zhang, H.; Chen, J.; Dong, S.; Fang, Y. Reversible regulation of CdTe quantum dots fluorescence intensity based on Prussian blue with high anti-fatigue performance. *Chem. Commun.* **2019**, *55*, 644–647.
- (5) Beneduci, A.; Cospito, S.; La Deda, M.; Veltri, L.; Chidichimo, G. Electrofluorochromism in  $\pi$ -Conjugated Ionic Liquid Crystals. *Nat. Commun.* **2014**, *5*, No. 3105.
- (6) Woodward, A. N.; Kolesar, J. M.; Hall, S. R.; Saleh, N.-A.; Jones, D. S.; Walter, M. G. Thiazolothiazole Fluorophores Exhibiting Strong Fluorescence and Viologen-Like Reversible Electrochromism. *J. Am. Chem. Soc.* **2017**, *139*, 8467–8473.

- (7) Kim, D.; Kwon, J. E.; Park, S. Y. Fully Reversible Multistate Fluorescence Switching: Organogel System Consisting of Luminescent Cyanostilbene and Turn-On Diarylethene. *Adv. Funct. Mater.* **2018**, *28*, 1706213–1706219.
- (8) Wang, Z.; Zhu, M.; Gou, S.; Pang, Z.; Wang, Y.; Su, Y.; Huang, Y.; Weng, Q.; Schmidt, O. G.; Xu, J. Pairing of Luminescent Switch with Electrochromism for Quasi-Solid-State Dual-Function Smart Windows. *ACS Appl. Mater. Interfaces* **2018**, 31697.
- (9) Thomas, S. W.; Joly, G. D.; Swager, T. M. Chemical sensors based on amplifying fluorescent conjugated polymers. *Chem. Rev.* **2007**, *107*, 1339–1386.
- (10) Jares-Erijman, E. A.; Jovin, T. M. FRET Imaging. *Nat. Biotechnol.* **2003**, *21*, 1387–1395.
- (11) Bakalova, R.; Zhelev, Z.; Aoki, I.; Ohba, H.; Imai, Y.; Kanno, I. Silica-Shell Single Quantum Dot Micelles as Imaging Probes with Dual or Multimodality. *Anal. Chem.* **2006**, *78*, 5925–5932.
- (12) Hecht, S.; Frechet, J. M. J. Dendritic encapsulation of function: applying nature's site isolation principle from biomimetics to materials science. *Angew. Chem., Int. Ed.* **2001**, *40*, 74–91.
- (13) Wang, J.; Zhao, Y.; Dou, Y. C.; Sun, H.; Xu, P.; Ye, K.; Zhang, J.; Jiang, S.; Li, F.; Wang, Y. Alkyl and dendron substituted quinacridones: synthesis, structures, and luminescent properties. *J. Phys. Chem. B* **2007**, *111*, 5082–5089.
- (14) Chen, L.; Xu, S.; McBranch, D.; Whitten, D. Tuning the properties of conjugated polyelectrolytes through surfactant complexation. *J. Am. Chem. Soc.* **2000**, *122*, 9302–9303.
- (15) Lim, S.-F.; Friend, R. H.; Rees, I. D.; Li, J.; Ma, Y.; Robinson, K.; Holms, A. B.; Hennebicq, E.; Beljonne, D.; Cacialli, F. Suppression of Green Emission in a New Class of Blue-Emitting Polyfluorene Copolymers with Twisted Biphenyl Moieties. *Adv. Funct. Mater.* **2005**, *15*, 981–988.
- (16) Kulkarni, A. P.; Jenekhe, S. A. Blue light-emitting diodes with good spectral stability based on blends of poly(9,9-dioctylfluorene): interplay between morphology, photophysics, and device performance. *Macromolecules* **2003**, *36*, 5285–5296.
- (17) Nguyen, B. T.; Gautrot, J. E.; Ji, C.; Brunner, P.-L.; Nguyen, M. T.; Zhu, X. X. Enhancing the photoluminescence intensity of conjugated polycationic polymers by using quantum dots as antiaggregation reagents. *Langmuir* **2006**, *22*, 4799–4803.
- (18) Luo, J.; Xie, Z.; Lam, J. W. Y.; Cheng, L.; Chen, H.; Qiu, C.; Kwok, H. S.; Zhan, X.; Liu, Y.; Zhu, D.; Tang, B. Z. Aggregation-induced emission of 1-methyl-1, 2, 3, 4, 5-pentaphenylsilole. *Chem. Commun.* **2001**, 1740–1741.
- (19) Mei, J.; Hong, Y.; Lam, J. W. Y.; Qin, A.; Tang, Y.; Tang, B. Z. Aggregation-Induced Emission: The Whole Is More Brilliant than the Parts. *Adv. Mater.* **2014**, *26*, 5429–5479.
- (20) Ding, D.; Li, K.; Liu, B.; Tang, B. Z. Bioprobes Based on AIE Fluorogens. *Acc. Chem. Res.* **2013**, *46*, 2441–2453.
- (21) Chi, Z.; Zhang, X.; Xu, B.; Zhou, X.; Ma, C.; Zhang, Y.; Liu, S.; Xu, J. Recent Advances in Organic Mechanofluorochromic Materials. *Chem. Soc. Rev.* **2012**, *41*, 3878–3896.
- (22) Fang, X.; Zhang, Y.; Chang, K.; Liu, Z.; Su, X.; Chen, H.; Zhang, S. X.-A.; Liu, Y.; Wu, C. Facile Synthesis, Macroscopic Separation, E/Z Isomerization, and Distinct AIE properties of Pure Stereoisomers of an Oxetane-Substituted Tetraphenylethene Lumino-gen. *Chem. Mater.* **2016**, *28*, 6628–6636.
- (23) Sun, N.; Tian, X.; Hong, L.; Su, K.; Zhou, Z.; Jin, S.; Wang, D.; Zhao, X.; Zhou, H.; Chen, C. Highly stable and fast blue color/fluorescence dual-switching polymer realized through the introduction of ether linkage between tetraphenylethylene and triphenylamine units. *Electrochim. Acta* **2018**, *284*, 655–661.
- (24) Mi, S.; Wu, J.; Liu, J.; Xu, Z.; Wu, X.; Luo, G.; Zheng, J.; Xu, C. AIEE-Active and Electrochromic Bifunctional Polymer and a Device Composed thereof Synchronously Achieve Electrochemical Fluorescence Switching and Electrochromic Switching. *ACS Appl. Mater. Interfaces* **2015**, *7*, 27511–27517.
- (25) Schmatz, B.; Ponder, J. F., Jr.; Reynolds, J. R. Multifunctional Triphenylamine Polymers Synthesized via Direct (Hetero) Arylation Polymerization. *J. Polym. Sci., Part A: Polym. Chem.* **2018**, *56*, 147–153.
- (26) Ning, Z.; Tian, H. Triarylamine: a promising core unit for efficient photovoltaic materials. *Chem. Commun.* **2009**, 5483–5495.
- (27) Li, W.; Pan, Y.; Xiao, R.; Peng, Q.; Zhang, S.; Ma, D.; Li, F.; Shen, F.; Wang, Y.; Yang, B.; Ma, Y. Employing ~100% Excitons in OLEDs by Utilizing a Fluorescent Molecule with Hybridized Local and Charge-Transfer Excited State. *Adv. Funct. Mater.* **2014**, *24*, 1609–1614.
- (28) Yen, H.-J.; Liou, G.-S. Solution-Processable Triarylamine-Based Electroactive High Performance Polymers for Anodically Electrochromic Applications. *Polym. Chem.* **2012**, *3*, 255–264.
- (29) Sun, N.; Meng, S.; Zhou, Z.; Chao, D.; Yu, Y.; Su, K.; Wang, D.; Zhao, X.; Zhou, H.; Chen, C. Electroactive (A<sub>3</sub><sup>+</sup> B<sub>2</sub>)-Type Hyperbranched Polyimides with Highly Stable and Multistage Electrochromic Behaviors. *Electrochim. Acta* **2017**, *256*, 119–128.
- (30) Hsiao, S.-H.; Cheng, S.-L. New Electroactive and Electrochromic Aromatic Polyamides with Ether-Linked Bis(triphenylamine) Units. *J. Polym. Sci., Part A: Polym. Chem.* **2015**, *53*, 496–510.
- (31) Quinton, C.; Alain-Rizzo, V.; Dumas-Verdes, C.; Miomandre, F.; Clavier, G.; Audebert, P. Redox-Controlled Fluorescence Modulation (Electrofluorochromism) in Triphenylamine Derivatives. *RSC Adv.* **2014**, *4*, 34332–34342.
- (32) Sun, N.; Meng, S.; Chao, D.; Zhou, Z.; Du, Y.; Wang, D.; Zhao, X.; Zhou, H.; Chen, C. Highly Stable Electrochromic and Electrofluorescent Dual-Switching Polyamide Containing Bis(diphenylamino)-fluorene Moieties. *Polym. Chem.* **2016**, *7*, 6055–6063.
- (33) Weng, D.; Shi, Y.; Zheng, J.; Xu, C. High Performance Black-to-Transmissive Electrochromic Device with Panchromatic Absorption Based on TiO<sub>2</sub>-Supported Viologen and Triphenylamine Derivatives. *Org. Electron.* **2016**, *34*, 139–145.
- (34) Sun, N.; Zhou, Z.; Chao, D.; Chu, X.; Du, Y.; Zhao, X.; Wang, D.; Chen, C. Novel aromatic polyamides containing 2-diphenylamino-(9,9-dimethylamine) units as multicolored electrochromic and high-contrast electrofluorescent materials. *J. Polym. Sci., Part A: Polym. Chem.* **2017**, *55*, 213–222.
- (35) Wałęsa-Chorab, M.; Skene, W. G. Visible-to-NIR Electrochromic Device Prepared from a Thermally Polymerizable Electroactive Organic Monomer. *ACS Appl. Mater. Interfaces* **2017**, *9*, 21524–21531.
- (36) Abraham, S.; Mangalath, S.; Sasikumar, D.; Joseph, J. Transmissive-to-Black Electrochromic Devices Based on Cross-Linkable Tetraphenylethene-Diphenylamine Derivatives. *Chem. Mater.* **2017**, *29*, 9877–9881.
- (37) Sun, N.; Su, K.; Zhou, Z.; Ye, Y.; Tian, X.; Wang, D.; Zhao, X.; Zhou, H.; Chen, C. AIE-Active Polyamide Containing Diphenylamine-TPE Moiety with Superior Electrofluorochromic Performance. *ACS Appl. Mater. Interfaces* **2018**, *10*, 16105–16112.
- (38) Lambert, C.; Nöll, G. The class II/III transition in triarylamine redox systems. *J. Am. Chem. Soc.* **1999**, *121*, 8434–8442.
- (39) Yen, H.-J.; Liou, G.-S. Solution-Processable Novel Near-Infrared Electrochromic Aromatic Polyamides Based on Electroactive Tetraphenyl-p-Phenylenediamine Moieties. *Chem. Mater.* **2009**, *21*, 4062–4070.
- (40) Liou, G.-S.; Chang, C.-W. Highly Stable Anodic Electrochromic Aromatic Polyamides Containing N, N', N'-Tetraphenyl-p-Phenylenediamine Moieties: Synthesis, Electrochemical, and Electrochromic Properties. *Macromolecules* **2008**, *41*, 1667–1674.
- (41) Brown, C. L.; Muderawan, I. W.; Young, D. J. High-pressure synthesis of oligoanilines. *Synthesis* **2003**, *16*, 2511.
- (42) Duan, X.-F.; Zeng, J.; Lü, J.-W.; Zhang, Z.-B. Insights into the General and Efficient Cross McMurry Reactions between Ketones. *J. Org. Chem.* **2006**, *71*, 9873–9876.
- (43) Yamazaki, N.; Higashi, F.; Kawabata, J. Studies on Reactions of the N-Phosphonium Salts of Pyridines. XI. Preparation of Polypeptides and Polyamides by Means of Triaryl Phosphites in Pyridine. *J. Polym. Sci., Polym. Chem. Ed.* **1974**, *12*, 2149–2154.
- (44) Wu, J. H.; Liou, G. S. High-Performance Electrofluorochromic Devices Based on Electrochromism and Photoluminescence-Active

Novel Poly (4-Cyanotriphenylamine). *Adv. Funct. Mater.* **2014**, *24*, 6422–6429.

(45) Cheng, S.-W.; Han, T.; Huang, T.-H.; Tang, B.-Z.; Liou, G.-S. High-performance electrofluorochromic devices based on aromatic polyamides with AIE-active tetraphenylethene and electro-active triphenylamine moieties. *Polym. Chem.* **2018**, *9*, 4364–4373.

(46) Yen, H.-J.; Liou, G.-S. Recent advances in triphenylamine-based electrochromic derivatives and polymers. *Polym. Chem.* **2018**, *9*, 3001–3018.

(47) Mei, J.; Leung, N. L. C.; Kwok, R. T. K.; Lam, J. W. Y.; Tang, B. Z. Aggregation-Induced Emission: Together We Shine, United We Soar! *Chem. Rev.* **2015**, *115*, 11718–11940.